PH. COLOMBAN

Raman spectrometry, a unique tool to analyze and classify ancient ceramics and glasses

Groupe des Nanophases et Solides Hétérogènes, Laboratoire Dynamique, Interactions et Réactivité, UMR 7075 CNRS and Université Pierre et Marie Curie, 2 rue Henry-Dunant, 94320 Thiais, France

ABSTRACT Raman micro/macro spectroscopy allows a non-destructive remote analysis: body and glaze, crystalline and amorphous phases can be identified, including the nanosized pigments coloring the glaze. Last-generation instruments are portable, which allows examination in museums, on archaeological sites, etc. This paper gives an overview of the potential of the Raman-spectrometry technique to analyze ancient ceramics and glasses. Selected glasses as well as glazes of various porcelains, celadons, faiences and potteries, representative of the different production technologies used in the Ancient, European, Mediterranean, Islamic and Asian worlds, were studied. Their identification is based on the study of the Raman fingerprint of crystalline and glassy phases. Raman parameters allow for the classification as a function of composition and/or processing temperature. Special attention is given to the spectra of amorphous and coloring phases (pigments).

PACS 81.05.Kf; 81.70.Fy; 81.05.Je; 01.65.+g

1 Introduction

Leading experts generally base their certification of ancient artifacts on stylistic analysis and on a personal feeling involving the five senses, but more objective proofs are mandatory for identification purposes. We demonstrate the potential of Raman spectroscopy as a non-destructive technique for the characterization of ceramics and glasses [1, 3]. Salient features can be extracted from bodies, glazes and pigments from different productions, evidencing artifacts covering the history of the ceramic industry: Sa Huynh culture potteries (> 3000 BP) [4], Punic/Roman time glasses (2nd BC to AD) [5], stonewares, celadons and porcelains from Vietnam (6th–16th centuries) [4, 6–9], soft- and hard-paste porcelains from Europe (18th–20th centuries) [10–13] and faiences or pottery from the Islamic world (Ifriqiya [14], Persia [15], Samarkand and the Silk Road [1, 16] and Turkey [17] (11th to 17th centuries)).

A ceramic is an artificial rock obtained by firing mixed raw materials together, which are more or less transformed by the thermal treatment. Ancient ceramics are composites at the typical scale of 5–500 µm and their microstructure consists of sintered grains of different compositions. Raw materials are almost fully molten to produce a glass or a glaze, but small crystals (< 0.1 µm to keep optical clearness) precipitate on cooling in many glasses. A (small) part of the ceramic itself is also molten during the firing process of the ceramic body and forms glassy phases on cooling. On the other hand, unreacted, incompletely dissolved raw materials as well as some phases formed during the process are crystalline. Different kinds of products are obtained if different technologies are applied to the same starting batch or if a given technology is applied to raw materials processed differently. Moreover, different technologies will often give products of very similar outward appearances (from the visual and sensory points of view), although these products are completely different in their micro/nanostructure. Yet, much information on the process remains written in the sample and the non-destructive Raman analysis of the microstructure (for ceramics) and nanostructure (for glasses and enamels) offers a way to identify it and, sometimes, to date ancient artifacts.

2 Experimental procedure

Raman spectroscopy is an optical technique and it thus can be performed through different optical devices: camera lenses, microscopes, remote fiber optic probes, etc. The size of the laser beam determines the surface analyzed in one shot. In a macro configuration, 100 to 500 µm² are illuminated, typically. The laser spot is reduced to ∼ 1 µm² for measurements with long-focus, high-magnification microscope objectives. Specific analysis of overpainting décor, glaze, underglaze décor and glaze/body interface can be made from the top using long-focus microscope objectives to restrain light penetration (Fig. 1a). An example is given with a lustre pottery: Fig. 1b shows the spectra of the over- and underglaze layers (the latter with cassiterite signature) recorded with green excitation and the spectra recorded in different points of the very surface of the lustre (red excitation). On the other hand, body analysis can be performed on glazed or unglazed regions (rim, bottom or support spurs). A good technique is to map the sample surface using an XY motorized platter, hence selecting the most representative spectra of the different constituents [13]. The choice of the exciting radiation must be optimized. Blue or violet (short-

✉ Fax: +33-14978-1118, E-mail: colomban@glvt-cnrs.fr
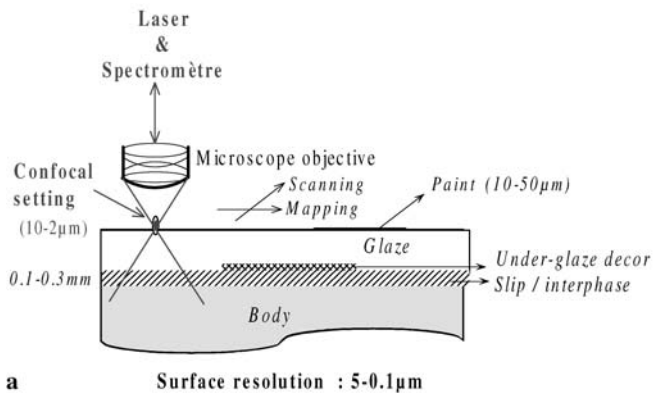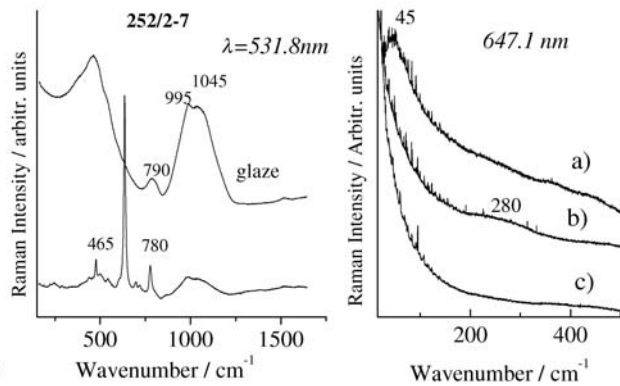
FIGURE 1 **a** Sketch of the Raman analysis of a ceramic; **b** example of lustreware analyses down from the glaze surface on Termez, Uzbekistan (*left*) and Fostât, Egypt (*right*) samples

FIGURE 2 Examples of phases/technology relationship; **a** in the body, mullite (M) for hard-paste porcelain (Meissen, Saxony, 19th century), β-wollastonite (W) and calcium phosphate (P) for soft-paste porcelains (Saint-Cloud and Chantilly, France, 18th century) and **b** in the glaze [13]; **c** comparison between a genuine Vietnamese celadon and a modern copy [16]
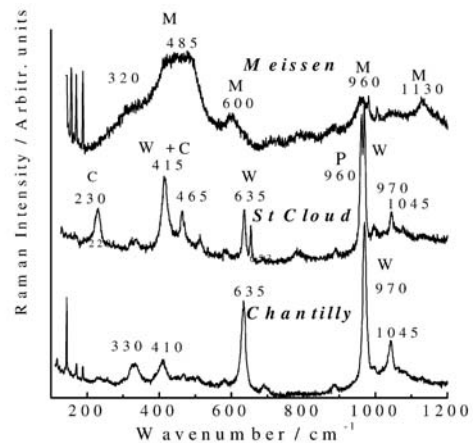
wavelength) excitation promotes a strong Raman scattering and provides a large spectral window with multichannel spectrographs, whereas red light must be preferred to analyze the low-wavenumber region, below $200 \, cm^{-1}$, specifically. The power of illumination needs to be reduced for colored glazes if the excitation energy corresponds to the chromophore electronic absorption (resonance Raman spectra [12, 15]), which induces local heating, and can modify the material through phase transition, oxidation or burning. Sometimes, fluorescence is observed, for instance for excavated samples. The reliability of the technique has been extensively discussed [7].
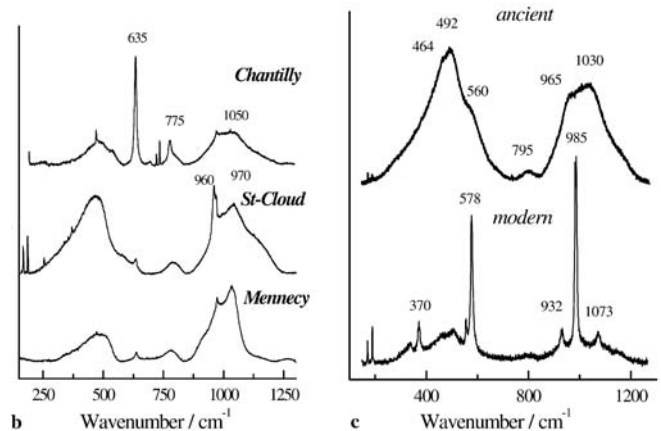
3 Results and discussion

3.1 *Information extracted from the Raman spectra*

The following information is present in the Raman spectra:

i) Nature of phases: identification of phases and polymorphs is very easily obtained from databases ([11, 18–20] and references therein) or references analyzed simultaneously by X-ray diffraction (XRD) [12]. Examples are given by the comparison between typical 18th-century hard- and soft-past porcelains or between an original Vietnamese celadon and its copy (Fig. 2). Note, however, that because the Raman cross section is directly related to the number of electrons involved in the (covalent) bond, some phases like rare nanosized precipitates of colored pigments are easily observed in Raman spectroscopy while they are not even visible by XRD. On the other hand, some main

phases can hardly be observed in Raman spectroscopy (e.g. tridymite).

ii) The structure and composition of glassy phases. For instance, Fig. 3a highlights the similarity between the glass of a Punic/Roman bead [5] and the glaze coating of a 'Lâj-vardina' ceramic [15].

3.2 *Identification from the spectra of crystalline phases*

The easy discrimination between soft- and hard-paste porcelain bodies (Fig. 2a) results from the high peak intensity of β-wollastonite ($CaSiO_3$, main band at $\sim 970 \, cm^{-1}$) and/or calcium phosphate (β-$Ca_3(PO_4)_2$, $\sim 960 \, cm^{-1}$) phases in soft pastes, while these phases are absent in hard paste [10, 11, 13]. On the other hand, mullite or mullite-like glassy phase spectra (main bands at ~ 480, 960 and $1130 \, cm^{-1}$) are observed in high-temperature-fired hard-paste porcelains (prepared with kaolin and feldspars) [10–13]. Discrimination is also possible with the signature of the precipitates in the glaze. Figure 2b shows representative Raman spectra recorded on the glazes from the three main factories in the Paris area in the 18th century: Chantilly, Mennecy and Saint-Cloud. Identification is obvious from the comparison of the crystalline phases both in the body and in the glaze or at
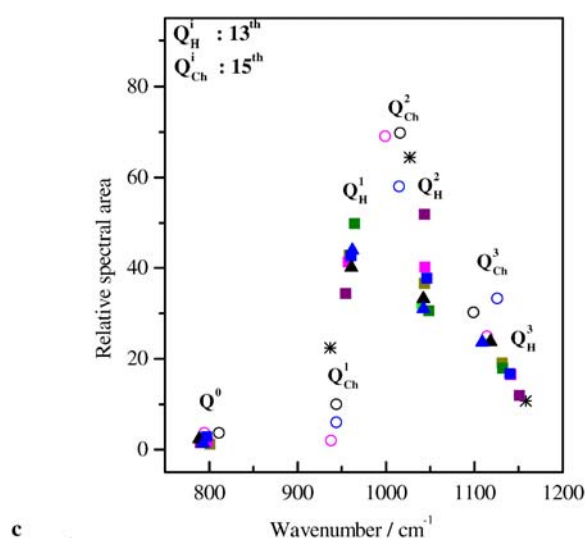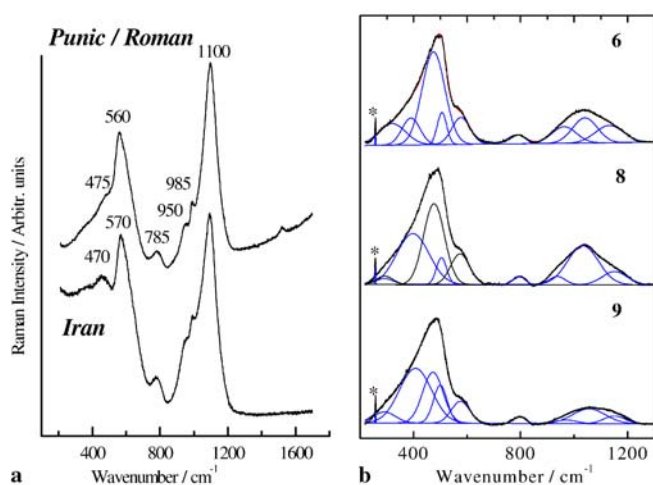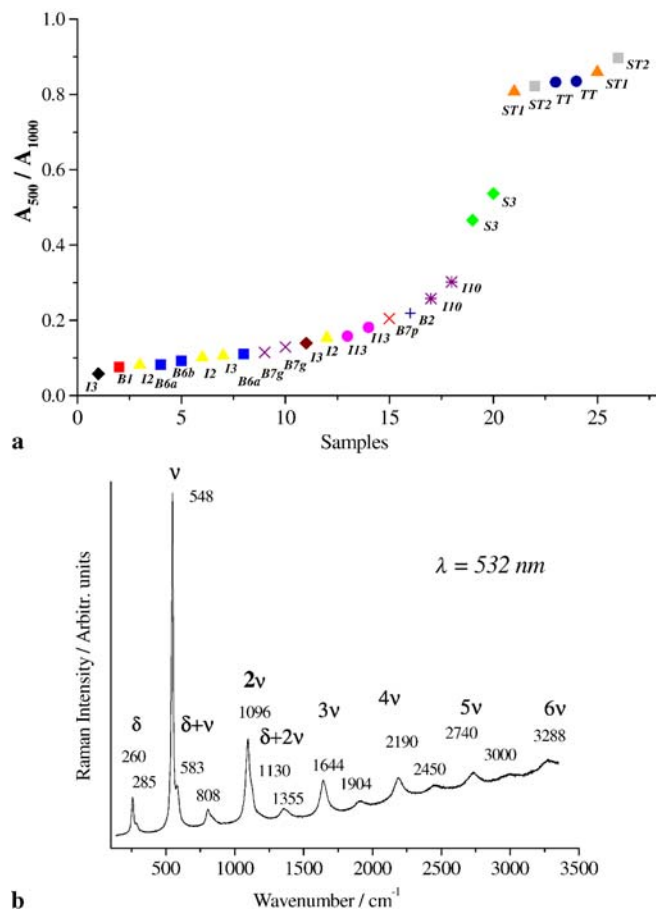
FIGURE 3 **a** Comparison of spectra recorded on a Punic/Roman glass bead ($\sim$ 2nd BC/AD, Carthage) [5] and a blue-glazed Lâjvardina ewer (13th century, Iran) [15]; **b** example of Si–O bending ($\sim$ 500 cm^{-1}) and stretching ($\sim$ 1000 cm^{-1}) Q_n components for hard-paste porcelain glazes with different compositions; **c** centers of gravity and relative areas of the Q_n components extracted from the Raman spectra recorded normal to the glaze surface (*squares*) and across the shard section (*triangles*) of the 13th-century celadon (*solid labels*) and the 15th-century porcelain (*open labels*) [7]

FIGURE 4 **a** The polymerization index is calculated from the area ratio of Si–O bending (A_{500}) and stretching (A_{1000}) envelopes; the samples are glazes from Byzantine (6th–15th centuries (B)) and Seljukides (11th–13th centuries) wares and tiles (from Iznik (I), Tokat (TT), Sivas (S & ST), Turkey [17]); **b** lapis lazuli resonance Raman spectrum recorded at the body/glaze interface in a Lâjvardina ceramic (13th century, Iran, see Fig. 3a)

the glaze/body interface [13]. In Fig. 2c, the Raman spectra obtained from modern and ancient Vietnamese celadons are compared. The narrow peaks of modern celadon spectra correspond to crystalline 'α'-wollastonite, $CaSiO_3$, in the glaze (main bands at $\sim$ 985 and 580 cm^{-1}). Examination of ancient celadons under a microscope shows that bubbles several tens of micrometers in size are almost homogeneously distributed in the glaze [8, 9]. These micrometer-size bubbles are an alternative to the precipitation of α-wollastonite to achieve a deep translucence. Chromium traces in the wollastonite give a green color, whereas the jade-like color is obtained from iron doping in the amorphous glaze of ancient celadons.

3.3   *Identification from the spectra of amorphous silicates. Relationship between processing and Raman spectra*

Glass and glaze can be fired at temperatures ranging from $\sim$ 600 °C (for instance for pottery lustre) to 1450 °C

(high-temperature-fired porcelain glaze). Glasses are silicate networks in which SiO_4 tetrahedra are bound together through oxygen atoms [19–22]. The properties change if these connections are modified by the incorporation of lead, alkali-earth/alkali elements, etc. By comparing Raman spectra of glassy (or crystalline) silicates, it clearly appears that the Raman intensity of Si–O bending and stretching envelopes varies with composition. The different components give information on the glass composition and structure [2, 3, 7, 10, 22]. A clear differentiation (comparison) is possible because the connectivity of the SiO_4 polymeric units can be investigated through the relative intensities of the components of the Si–O stretching and bending modes at $\sim$ 1000 and 500 cm^{-1}, respectively (see the similarity of two different glazes in Fig. 2a and typical decompositions in Fig. 3b) [7].

Figure 4a compares the A_{500}/A_{1000} polymerization index (with A_{500} being the Raman area of the 500-cm^{-1} band and A_{1000} being the Raman area of the 1000-cm^{-1} band) for a series of samples from Turkey (Byzantine to Seldjukide periods) [17]. The relationship between the Raman index of polymerization and both the glass composition and the temperature of processing is well documented [3, 22]: the first family ($A_{500}/A_{1000} < 0.3$) mostly corresponds to Islamic

lead-containing or lustre potteries and some Punic/Roman glasses; the second family ($0.3 < A_{500}/A_{1000} < 0.8$) consists of some 19th-century lead-based soft-paste porcelain enamels and some Punic/Roman glasses (blue, green and colorless); the third family ($0.8 < A_{500}/A_{1000} < 1.1$) corresponds to most ancient glasses and the 18th-century soft-paste porcelain enamels; family no. 4 corresponds to celadon Ca-based enamels and family no. 5 to Ca-based porcelain enamels. Family no. 6 corresponds to K-based hard-paste porcelain glaze. The A_{500}/A_{1000} ratio is strongly correlated to the processing temperature (from $\sim 1400\,°C$ for $A_{500}/A_{1000} \sim 7$, $1000\,°C$ for $A_{500}/A_{1000} \sim 1$ and $\sim 600\,°C$ or less for $A_{500}/A_{1000} \sim 0.3$). Because the SiO_4 tetrahedron is a very well defined vibrational and structural entity, its different configurations have specific vibrational fingerprints. From the literature [7, 10, 21, 22] the different spectral components of the stretching envelope (Fig. 3b) were assigned to the silica vibrations with zero (Q^0 or isolated SiO_4), one (Q^1 or dumbbell $-SiO_3$), two (Q^2 or $= SiO_2$), and three (Q^3 or $\equiv SiO$) bridging oxygens (or equivalent to the four, three, two and one non-bridging oxygens) per tetrahedral group, respectively. Q^4 corresponds to fully polymerized tetrahedra as in pure silica. Decomposition of the bending and stretching massifs is illustrated with the example of Vietnamese ceramics given in Fig. 3c [7]: a clear differentiation between two kiln productions from the 13th and 15th centuries is obvious for Q^1, Q^2 and undifferentiated Q^{3-4} components.

3.4   *Pigments and resonance Raman spectroscopy*

The size of the crystalline pigments dispersed in glassy coatings must be around or just below 100 nm to obtain a high-gloss glaze. Pigments are thus among the oldest materials for which the nanocrystalline state has to be tailored. For a given coloring ion, the result depends on the glaze composition, the firing temperature, the atmosphere and the grinding. In other words, the final color depends on the technology used.

The different ways of coloring matrices will produce different Raman features [11]:

i)   Dispersion of transition-metal ions (Cu^{2+}, $Co^{2+\,or\,3+}$, $Mn^{2+\,or\,3+}$, ...) in the glassy coating. In this case, the Raman scattering will not be very sensitive;

ii) precipitation of 'small' (colored) crystals on cooling. This technique is widely used to opacify the matrix (e.g. cassiterite (SnO_2) in Figs. 1b and 2b). The small size of the crystals leads to a characteristic band broadening in the Raman spectrum;

iii) dispersion of an insoluble colored crystal (a pigment) in the coating matrix with a very characteristic Raman fingerprint [11];

iv) dispersion of metal nanoparticles like gold (Cassius purple), silver or copper (lustreware). This gives very low wavenumber features (Fig. 1b).

Note that because pigments are colored, some resonance effects can occur, in which case the Raman spectra will depend on the exciting light and the chromophore amount [11, 12]. See, for instance, the spectrum of lapis lazuli in Fig. 4b:

the fundamental bands related to S_n chromophores at ~ 260 and $548\,cm^{-1}$ give rise to harmonics ($n\nu$) and combinations ($\delta + n\nu$) [15]. A very low wavenumber contribution also appears ($20–60\,cm^{-1}$, Fig. 1b) associated with Cu/Ag metal precipitates (and their ions) at the origin of the metallic lustre [23].

4   Conclusion

Macro- and micro-Raman spectroscopy is a good tool for the non-destructive remote identification of glasses and ceramics, in spite of the small size, low crystallinity and/or low amount of the probed phases. A feasible discrimination has been demonstrated by considering the fingerprint of both crystalline and amorphous phases. Besides, extracting some parameters from the Raman spectra of amorphous silicates allows their classification as a function of composition (Pb-, Ca- or K-based) and/or processing temperature. Spectra of amorphous matrices colored by different (nano)crystalline phases allows for the identification of the pigment as well as the processing.

REFERENCES

1 Ph. Colomban: Asian Chem. Lett. **5**, 125 (2001)
2 Ph. Colomban: 'Glasses, Glazes and Ceramics – Recognition of the Ancient Technology from the Raman Spectra, Raman Spectroscopy'. In: *Archaeology and Art History*, ed. by H.G.M. Edwards, J.M. Chalmers (Royal Society of Chemistry, London 2004) in press
3 Ph. Colomban: Actual. Chim., 12 février (2003)
4 Ph. Colomban, D.N. Khoi, N.Q. Liem, C. Roche, G. Sagon: J. Cult. Heritage (2004), in press
5 Ph. Colomban, G. March, L. Mazerolles, T. Karmous, N. Ayed, A. Ennabli, H. Slim: J. Raman Spectrosc. **34**, 205 (2003)
6 N.Q. Liem, G. Sagon, V.X. Quang, H.V. Tan, Ph. Colomban: J. Raman Spectrosc. **31**, 933 (2000)
7 N.Q. Liem, N.T. Thanh, Ph. Colomban: J. Raman Spectrosc. **33**, 287 (2002)
8 Ph. Colomban, G. Sagon, L.Q. Huy, N.Q. Liem, L. Mazerolles: Archaeometry **46**, 125 (2004)
9 Ph. Colomban, N.Q. Liem, G. Sagon, H.X. Tinh, T.B. Hoành: J. Cult. Heritage **4**, 197 (2003)
10 Ph. Colomban, F. Treppoz: J. Raman Spectrosc. **32**, 93 (2001)
11 Ph. Colomban, G. Sagon, X. Faurel: J. Raman Spectrosc. **32**, 351 (2001)
12 X. Faurel, A. Vanderperre, Ph. Colomban: J. Raman Spectrosc. **34**, 290 (2003)
13 Ph. Colomban, I. Robert, C. Roche, G. Sagon, V. Milande: Rev. Archéom., submitted
14 Ph. Colomban, G. Sagon, A. Louhichi, H. Binous, N. Ayed: Rev. Archéom. **25**, 101 (2001)
15 Ph. Colomban: J. Raman Spectrosc. **34**, 420 (2003)
16 Ph. Colomban, A. Collinet, M. Kervran: unpublished work
17 E.N. Caner-Saltik, Ph. Colomban, V. Soulet, S. Demirci, A. Türkmenoglu, S. Özcilingir-Akgün, Ö. Bakirer: 'Analysis of Anatolian medieval ceramic glazes XRD and Non-destructive Raman microSpectrometry', in *Proc. Archéométrie 2003, Bordeaux, 16–19 April 2003* p. 64
18 I.M. Bell, R.J.H. Clark, P.J. Gibbs: Spectrochem. Acta **53**, 2159 (1997)
19 W.P. Griffith: *Infrared and Raman Spectroscopy of Lunar and Terrestrial Minerals*, ed. by C. Karr Jr. (Academic, New York 1975) p. 197
20 M. Pinet, D.C. Smith, B. Lasnier: Rev. Gemmol. Hors Sér., 11 June (1992)
21 F. Seifert, B.O. Mysen, D. Virgo: Am. Mineral. **67**, 696 (1982)
22 Ph. Colomban: J. Non-Cryst. Solids **323**, 180 (2003)
23 Ph. Colomban, C. Truong: J. Raman Spectrosc. **35** (2004), in press